Finite Control Set Model Predictive Current Control of a Five-Phase PMSM with Virtual Voltage Vectors and Adaptive Control Set

Wusen Wang, Ying Fan, *Senior Member, IEEE*, Siyu Chen and Qiushi Zhang

***Abstract*—This paper presents an improved finite control set model predictive current control (FCS-MPCC) of a five-phase permanent magnet synchronous motor (PMSM). First, to avoid including all the 32 voltage vectors provided by a two-level five-phase inverter into the control set, virtual voltage vectors are adopted. As the third current harmonics can be much reduced by virtual voltage vectors automatically, the harmonic items in the cost function of conventional FCS-MPCC are not considered. Furthermore, an adaptive control set is proposed based on voltage prediction. Best control set with proper voltage vector amplitude corresponding to different rotor speed can be achieved by this method. Consequently, current ripples can be largely reduced and the system performs much better. At last, simulations are established to verify the steady and transient performance of the proposed FCS-MPCC, and experiments based on a 2 kW five-phase motor are carried out. The results have validated the performance improvement of the proposed control strategy.**

***Index Terms*—Adaptive control set, current ripple, finite control set model predictive current control (FCS-MPCC), permanent magnet synchronous motor (PMSM), virtual voltage vectors.**

I. Introduction

As an important role in multiphase machines, five-phase permanent magnet synchronous motors (PMSMs) have received much attention during the past decade [1-3]. Compared with three-phase PMSM, five-phase machines can achieve the advantages of lower torque ripples, better fault-tolerant capability and additional degrees of freedom regardless of slight control complexity [4]. Therefore, five-phase PMSM is more appropriate for high performance conditions like electric vehicles (EVs) traction.

Model predictive control (MPC) is a kind of advanced non-linear control algorithms for PMSM. Assuming that the motor is controlled by a voltage source inverter, MPC can optimize the voltage output based on the system model in real time. According to the difference of voltage output, MPC can be divided into two categories, continuous control set MPC (CCS-MPC) and finite control set MPC (FCS-MPC) [5-6]. CCS-MPC obtains the optimal voltage vector by taking derivative of the cost function so that any voltage vector under amplitude limit can be obtained by the inverter with pulse width modulation (PWM) [7-8]. FCS-MPC utilizes the discrete nature of inverters and usually enumerates all the alternative voltage vectors and chooses one best output based on the cost function [9-10]. Compared with CCS-MPC, FCS-MPC lists the gate status of the inverter corresponding to every voltage vector in the control set and controls the inverter directly without PWM. Hence, the executive process can be simplified.

However, in FCS-MPC, the control set is discrete. Different from synthesized vectors provided by PWM in CCS-MPC, which are unlimited in directions, only countable voltage vectors can be applied to the invertors. Consequently, the ripples in electromagnetic torque or stator current will be larger in FCS-MPC [11]. What's more, all voltage vectors in the control set of FCS-MPC should be judged by a cost function in every control interval, which will lead to a heavy computational burden for microcontroller compared with conventional control strategies like field orient control (FOC) or direct torque control (DTC). In multiphase motor control system, this issue will be more severe as the control set is larger [12-13]. Therefore, the main challenge of FCS-MPC is to reduce the torque ripple or current ripple as well as the computational burden.

To reduce ripples, a feasible way is to enlarge the control set, i.e., to increase voltage vectors. In [14], discrete space-vector modulation (DSVM) is introduced into a FCS-MPC system to offer more vectors to reduce torque ripple. Also, deadbeat-direct torque and flux control (DB-DTFC) is applied to obtain the location of the anticipating vector so that only three voltage vectors need to be concerned in every control interval rather than all in the control set. However, the usage of DB-DTFC increases the computational burden which nullifies the advantage of concerning only three vectors. In [15], a novel FCS-MPC algorithm is proposed with current locus and without cost function. The prediction is carried out with the zero-voltage vector only instead of all the vectors in the control set. As a result, the predicting time can be eliminated and computational burden is reduced. In the five-phase motor

This article was submitted for review on 31, January, 2018.

This work was supported in part by the National Natural Science Foundation of China under 61374125.

Wusen Wang is with the School of Electrical Engineering, Southeast University, Nanjing, JS 210096 China (e-mail: wangws215@qq.com).

Ying Fan is with the School of Electrical Engineering, Southeast University, Nanjing, JS 210096 China (e-mail: vickifan@seu.edu.cn).

Siyu Chen is with the School of Electrical Engineering, Southeast University, Nanjing, JS 210096 China (e-mail: ee_chensiyu@icloud.com).

Qiushi Zhang is with the School of Electrical Engineering, Southeast University, Nanjing, JS 210096 China (e-mail: zqs55@qq.com).

control, FCS-MPC with virtual voltage vectors is proposed in [16]. By adopting virtual voltage vectors, the third harmonics can be restrained automatically and only 11 voltage vectors need to be judged by cost function rather than 21 or even 31. However, constant amplitude of the vectors is not appropriated in all conditions, especially in low speed cases.

In this paper, an improved finite control set model predictive current control (FCS-MPCC) algorithm for five-phase PMSMs is proposed. Virtual voltage vectors are utilized in the algorithm although the third harmonic items of the cost function is not concerned and the cost function is simpler compared with [16]. Moreover, an adaptive control set method based on alterable amplitude voltage vectors is included in the algorithm to reduce the ripples in the stator current. This paper is organized as follows. In Section II, the model of five-phase PMSM and inverter are briefly introduced. Section III is where virtual voltage vectors and conventional FCS-MPCC are described. In Section IV, the proposed algorithm is analyzed in detail. And then, simulations and experimental results are presented in Section V. At last, conclusions are stated in Section VI.

II. Model of Five-Phase PMSM and Inverter

A. Model of Five-Phase PMSM

As the third harmonics is not included in the model predictive control in this paper, only fundamental model of the five-phase PMSM is discussed.

In the synchronous rotating d-q frame, the relationship between stator voltage v_d, v_q and current i_d, i_q can be presented as

$$\begin{aligned}\begin{bmatrix} v_d \\ v_q \end{bmatrix} &= R_s \cdot \begin{bmatrix} i_d \\ i_q \end{bmatrix} + \begin{bmatrix} L_d & 0 \\ 0 & L_q \end{bmatrix} \cdot \left(\frac{d}{dt} \begin{bmatrix} i_d \\ i_q \end{bmatrix} \right) \\ &+ \omega_e \cdot \left(\begin{bmatrix} -L_q & 0 \\ 0 & L_d \end{bmatrix} \cdot \begin{bmatrix} i_q \\ i_d \end{bmatrix} + \begin{bmatrix} 0 \\ \lambda_{pm} \end{bmatrix} \right)\end{aligned} \tag{1}$$

where R_s is stator phase resistance, L_d and L_q are inductance in d-axis and q-axis respectively, ω_e is rotor electric speed, and λ_{pm} is the flux linkage of permanent magnet.

In FCS-MPCC, the current prediction is based on motor model and is executed in every control interval. To support this, the motor model in (1) should be discretized. As the control interval T_s is often short enough, forward Euler derivative is used in the discretization to simplify the process. The discrete model of five-phase PMSM is

$$\begin{aligned}\begin{bmatrix} i_d(k+1) \\ i_q(k+1) \end{bmatrix} &= \begin{bmatrix} 1 - R_s T_s / L_d & T_s \omega_e(k) \\ -T_s \omega_e(k) & 1 - R_s T_s / L_q \end{bmatrix} \begin{bmatrix} i_d(k) \\ i_q(k) \end{bmatrix} \\ &+ \begin{bmatrix} T_s / L_d & 0 \\ 0 & T_s / L_q \end{bmatrix} \begin{bmatrix} v_d(k) \\ v_q(k) \end{bmatrix} - \begin{bmatrix} 0 \\ T_s \lambda_{pm} \omega_e(k) / L_q \end{bmatrix}\end{aligned}. \tag{2}$$

B. Model of Two-Level Five-Phase Inverter

In a two-level five-phase inverter, there are 32 kinds of switching state and hence 32 voltage vectors can be obtained in the fundamental plane as shown in Fig. 1(a). Every number represents a voltage vector output of two-level five-phase inverter. Meanwhile, the corresponding voltage vectors in the third harmonic plane are presented in Fig. 1(b).

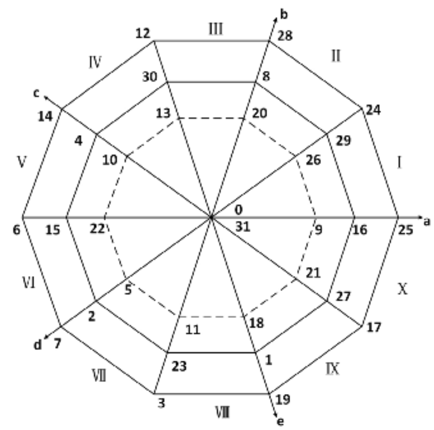

(a) Voltage vectors in fundamental plane

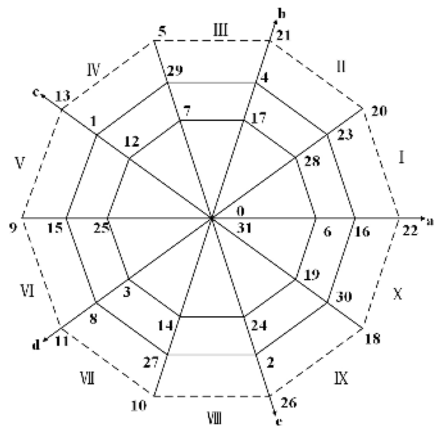

(b) Voltage vectors in third harmonic plane

Fig. 1. Voltage vectors provided by two-level five-phase inverter.

III. Conventional FCS-MPCC with Virtual Voltage Vectors

A. Virtual Voltage Vectors

In fundamental plane, Fig. 1(a), assuming that the DC voltage is U_{dc}, the vectors ending at the outermost decagon are the large vectors with the length of $0.6472 \cdot U_{dc}$, the vectors ending at the middle decagon are the middle vectors with the length of $0.4 \cdot U_{dc}$, and the innermost are the small vectors with the length of $0.2472 \cdot U_{dc}$. As shown in Fig. 1, it is fortunate that the large vectors and middle vectors in the fundamental plane change into small vectors and middle vectors respectively in the third harmonic plane. In addition, the large and middle vectors with the same direction in fundamental plane has the opposite direction when they become small and middle vectors in the third harmonic plane. Consequently, the synthesized voltage vector in the third harmonic plane can be limited to zero with appropriate control of the voltage vectors in the fundamental plane.

To guarantee that the voltage in the third harmonic plane is zero, small vectors in the fundamental plane are not included when gathering the control set of FCS-MPCC. Besides, the active time of large vectors T_{lar} and middle vectors T_{mid} should satisfy

$$T_{lar}/T_{mid} = 1.618\,. \tag{3}$$

Therefore, the voltage vectors in the fundamental plane can be simplified by using only 11 virtual voltage vectors with the amplitude of $0.5527 \cdot U_{dc}$, as shown in Fig. 2.

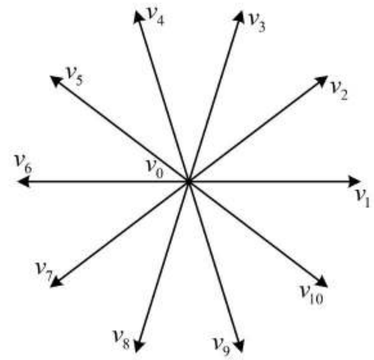

Fig. 2. Virtual voltage vectors in fundamental plane.

B. FCS-MPCC with Virtual Voltage Vectors

In conventional FCS-MPCC with virtual voltage vectors, the cost function is defined as

$$J = \left(i_{d1ref} - i_{d1}\right)^2 + \left(i_{q1ref} - i_{q1}\right)^2 + \left(i_{d3ref} - i_{d3}\right)^2 + \left(i_{q3ref} - i_{q3}\right)^2 \tag{4}$$

where i_{d1ref} and i_{q1ref} are current references in the fundamental plane, i_{d3ref} and i_{q3ref} are current references in the third harmonic plane, i_{d1} and i_{q1} are the predicted current in the fundamental plane, i_{d3} and i_{q3} are the predicted current in the third harmonic plane. The control set consists of 11 virtual voltage vectors. In every control interval, all the virtual voltage vectors are used to predict the next-interval current and are judged by (4), then the best vector are selected as the output of the inverter.

As the virtual voltage vectors can eliminate the third harmonic voltage automatically, there is no need to judge the third harmonic current in the cost function. Moreover, constant amplitude of voltage vectors cannot adapt in all conditions and can cause ripples in current or torque especially when rotor speed is low.

IV. Proposed FCS-MPCC

To modify FCS-MPCC in a five-phase motor control system, virtual voltage vectors are also utilized in this paper with the cost function optimally designed and the control set to be adaptive according to system state.

A. Delay Compensation

First of all, due to the discrete nature of FCS-MPCC and the real control system, sampling and computing will occupy some time and the derived control signal can drive the inverter only at next control interval. Consequently, one control interval delay exists and will cause vibration or even instability in the system.

To compensate the delay, system state at next control interval should be predicted before dealing with FCS-MPCC. The prediction can be carried out by using (2), in which $i_d(k)$, $i_q(k)$, $v_d(k)$, $v_q(k)$, and $\omega_e(k)$ are sampling results and $i_d(k+1)$ and $i_q(k+1)$ are the predicted stator current.

B. Cost Function

In FCS-MPCC, a cost function is used to judge the voltage vectors and determines the performance of the system. As the third harmonic voltage is reduced automatically by adopting virtual voltage vectors, there is no need to include third harmonic current items in the cost function. Therefore, the cost function in the proposed FCS-MPCC is

$$J = \left[i_{dref}(k+2) - i_d(k+2)\right]^2 + \left[i_{qref}(k+2) - i_q(k+2)\right]^2 \tag{5}$$

where, $i_{dref}(k+2)$ and $i_{qref}(k+2)$ are current references at $k+2$ control interval, $i_d(k+2)$ and $i_q(k+2)$ are the predicted current at $k+2$ control interval.

According to (2), the predicted current can be calculated by

$$\begin{aligned}\begin{bmatrix} i_d(k+2) \\ i_q(k+2) \end{bmatrix} &= \begin{bmatrix} 1 - R_s T_s/L_d & T_s\omega_e(k+1) \\ -T_s\omega_e(k+1) & 1 - R_s T_s/L_q \end{bmatrix}\begin{bmatrix} i_d(k+1) \\ i_q(k+1) \end{bmatrix} \\ &+ \begin{bmatrix} T_s/L_d & 0 \\ 0 & T_s/L_q \end{bmatrix}\begin{bmatrix} v_{dset} \\ v_{qset} \end{bmatrix} - \begin{bmatrix} 0 \\ T_s\lambda_{pm}\omega_e(k+1)/L_q \end{bmatrix}\end{aligned} \tag{6}$$

where, v_{dset} and v_{qset} are voltage vectors in the control set. As the control interval is short enough, rotor speed can be treated as a constant during a control interval. Therefore, $\omega_e(k+1) = \omega_e(k)$.

C. Adaptive Control Set

In a conventional FCS-MPCC with virtual voltage vectors, the voltage vectors in control set keep constant in amplitude, i.e., $0.5527 \cdot U_{dc}$. However, this is the largest voltage that a five-phase inverter can provide and when the rotor speed is small, the back electromotive force is also small, a voltage vector with the amplitude of $0.5527 \cdot U_{dc}$ will be too large that ripples will occur in the stator current. To solve the problem, the amplitude of the voltage vectors should be variable and adapt to different rotor speeds. A feasible way is to predict the voltage vector based on rotor speed and decide the amplitude of the voltage vectors in the control set before they are judged by the cost function.

First, the rotor direction at next control interval is predicted. As the rotor speed is constant during a control interval, the rotor direction at next control interval is

$$\theta_e(k+1) = \theta_e(k) + \omega_e(k) \cdot T_s \tag{7}$$

where, $\theta_e(k)$ and $\theta_e(k+1)$ are the rotor direction at current interval and next interval respectively.

Second, the voltage vector at next control interval is estimated by

$$\begin{aligned}\begin{bmatrix} v_{dest}(k+1) \\ v_{qest}(k+1) \end{bmatrix} &= \begin{bmatrix} R_s - L_d/T_s & -\omega_e(k)L_q \\ \omega_e(k)L_d & R_s - L_q/T_s \end{bmatrix}\begin{bmatrix} i_{dref}(k+1) \\ i_{qref}(k+1) \end{bmatrix} \\ &+ \begin{bmatrix} L_d/T_s & 0 \\ 0 & L_q/T_s \end{bmatrix}\begin{bmatrix} i_{dref}(k+2) \\ i_{qref}(k+2) \end{bmatrix} + \begin{bmatrix} 0 \\ \omega_e(k)\lambda_{pm} \end{bmatrix}\end{aligned} \tag{8}$$

and it can be transferred to stator α-β frame

$$\begin{aligned}&\begin{bmatrix} v_{\alpha est}(k+1) \\ v_{\beta est}(k+1) \end{bmatrix} \\ &= \begin{bmatrix} \cos(\theta_e(k+1)) & -\sin(\theta_e(k+1)) \\ \sin(\theta_e(k+1)) & \cos(\theta_e(k+1)) \end{bmatrix}\begin{bmatrix} v_{dest}(k+1) \\ v_{qest}(k+1) \end{bmatrix}\end{aligned}. \tag{9}$$

Then, the amplitude of the estimated vector is

$$v_{est}\left(k+1\right)=\sqrt{v_{\alpha est}\left(k+1\right)^{2}+v_{\beta est}\left(k+1\right)^{2}}\ . \tag{10}$$

Third, define that K is an adaptive factor,

$$K=v_{est}\left(k+1\right)/\left(0.5527\cdot U_{dc}\right). \tag{11}$$

All the virtual voltage vectors should multiply by K before they are judged by the cost function. And the adaptive control set is constructed. It should be clarified that the transfer from synchronous rotating d-q frame to stator α-β frame (9) is actually not necessary in real control system as the amplitude of voltage vectors will keep constant when doing the transfer. K can be calculated with the amplitude of voltage vectors in synchronous rotating d-q frame. The transfer (9) here is just to present a more logical derivation.

Besides, to guarantee the transient performance, when i_q reference reaches the limit, which means either the speed reference or the load torque is changed, the adaptive factor K should take an extra increment. For example, K is equal to one in transient state in this paper.

D. The Whole Proposed FCS-MPCC system

The proposed five-phase motor FCS-MPCC system, which contains a speed loop and a current loop, is presented in Fig. 3. The speed loop is controlled by PI regulator. The current loop is based on the proposed FCS-MPCC. First, stator current at next control interval is predicted and the adaptive control set is obtained. Second, the anticipated stator current produced by every voltage vector in adaptive control set is calculated. Finally, the anticipated current is judged by cost function and the best voltage vector is selected and output.

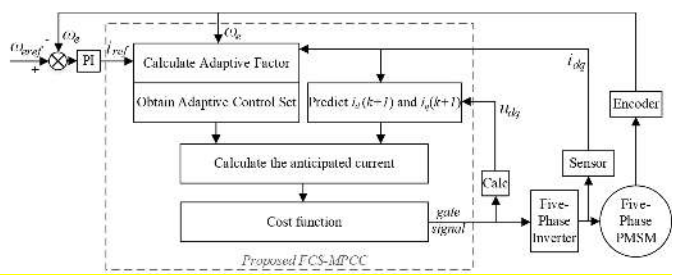

Fig. 3. The proposed five-phase motor FCS-MPCC system.

V. Simulation and Experimental Results

A. Simulation results

To simulate the proposed FCS-MPCC method of a five-phase PMSM, the model shown in Fig. 3 and the algorithm deduced in IV are established in MATLAB/Simulink. As a comparison, the conventional FCS-MPCC presented in [16] with virtual voltage vectors is also simulated. The coefficients of the speed loop PI regulators in both models are the same with K_p = 0.5 and K_i = 0.9. The d-axis current reference is zero and the q-axis current reference is the output of the PI regulators. The DC voltage is set to 150V. The parameters of the five-phase PMSM are listed in Table I.

Fig. 4 presents the simulation results of the conventional FCS-MPCC. Stator current in synchronous rotating d-q frame, i_d and i_q, phase current i_{abcde}, and rotor speed n are analyzed. Generally, ripples are obvious in the stator current. When the rotor speed is 300 r/min, i_d ranges from -0.6A to 0.7A and the THD of phase current is up to 20.2%. When rotor accelerates to 600 r/min, the ripples are reduced with i_d ranging from -0.4A to 0.5A and the THD of phase current down to 17.5%. It can be inferred that in the conventional FCS-MPCC, when rotor speed is low, the back electromotive force (EMF) is small, a voltage vector with an amplitude of $0.5527\cdot U_{dc}$ is too large to perform well. However, when the speed is increased, the back EMF becomes larger and a $0.5527\cdot U_{dc}$ voltage vector can perform better. In other words, a constant control set is not suitable for the motor in many cases especially when the rotor speed is low. However, at the transient state, conventional FCS-MPCC shows satisfying performance, i_q reference reaches the upper limit quickly and holds until rotor speed reaches the new reference.

Simulation results of the proposed FCS-MPCC are presented in Fig. 5. Compared with the results of the conventional method, the current ripple is reduced visibly. At 300 r/min, the ripple in i_d and i_q can be ignored and the THD of phase current is only 3.40%. At 600 r/min, ripples in i_d ranges from -0.05A to 0.25A, and is 66.6% smaller than that in the conventional method. The THD of the phase current increases a bit to 5.21%. Moreover, considering the transient performance of the proposed FCS-MPCC, when speed reference changes, i_q reference reached the upper limit just as the conventional method does. The transient performance of the proposed method is not weakened.

Table I
Parameters of the Five-Phase PMSM

Parameter	Value
Rated Power	2 kW
Stator resistance	0.5 Ω
Rate rotor speed	1500 r/min
Rated torque	12 N·m
d-axis inductance	12.4 mH
q-axis inductance	14.3 mH
Flux linkage of PM	0.09 Wb
Rotational inertia	0.006 kg·m^2
Friction factor	0.02 N·m·s/rad

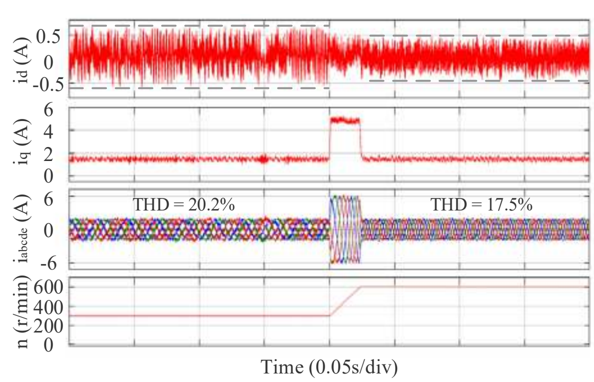

Fig. 4. Simulation results of conventional FCS-MPCC.

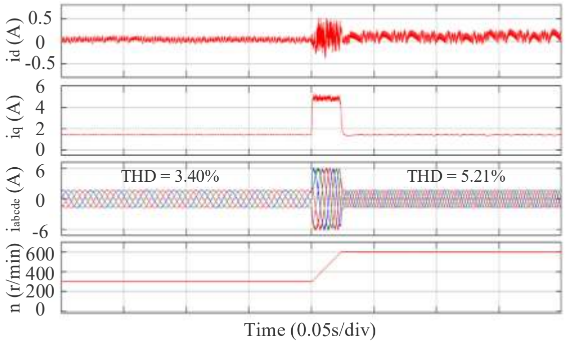

Fig. 5. Simulation results of the proposed FCS-MPCC.

B. Experimental results

To further verify the performance of the proposed FCS-MPCC method, an experimental platform is constructed with dSPACE1104. The system is shown in Fig. 6. The platform contains a five-phase PMSM, a magnetic brake, a dSPACE-computer control system, an inverter, an oscilloscope and other necessary devices. To make comparison, conventional FCS-MPCC is also experimental implemented. The only difference of this two experiments is whether an adaptive control set is included. The speed loop PI regulator, DC voltage, control interval and load torque are the same. Especially, the coefficients of the speed loop PI are $K_p = 0.5$ and $K_i = 0.9$, the DC voltage is 150V, the control interval is 100us and the load torque is 7N·m.

Fig. 7 shows the steady state of the conventional FCS-MPCC and the proposed one. The rotor speed is 300 r/min. In conventional algorithm, the ripples in i_d and i_q are more than 1A and there is some vibration in current. In the proposed method, the ripples in i_d and i_q are about 0.5A, and the system is stable with no vibration. Therefore, the performance improvement of the proposed predictive control is further verified. So when the motor is operating at a low speed, a control set with voltage vectors based on full DC voltage is not appropriate. The adaptive control set corresponding to rotor speed can provide performance improvement for FCS-MPCC.

The experimental results of transient state are presented in Fig. 8. The rotor speed changes from 300 r/min to 600 r/min, and the DC voltage is kept 150V. It can be confirmed that both the proposed FCS-MPCC and the conventional method spend 80ms reaching the new speed reference. The extra increased adaptive factor is feasible to improve the transient performance. Besides, at 600 r/min, the current ripples in the proposed FCS-MPCC are also smaller than that in the conventional method, further validating the steady performance.

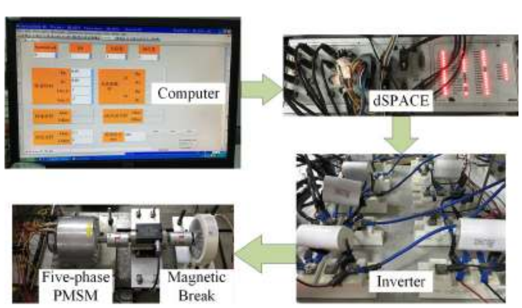

Fig. 6. Experimental platform of FCS-MPCC.

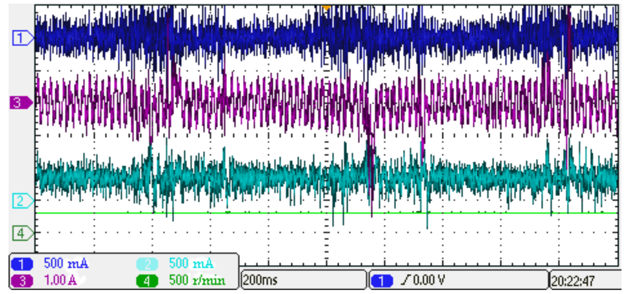

(a) Conventional FCS-MPCC

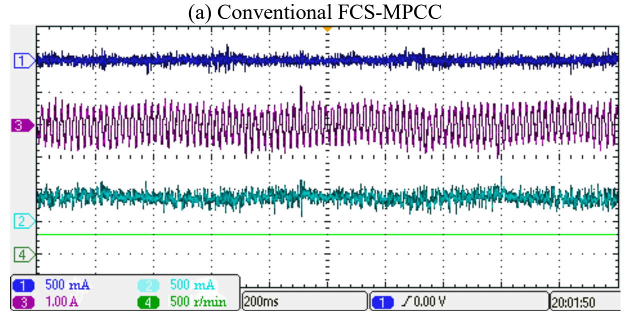

(b) Proposed FCS-MPCC.

Fig. 7. Experimental results at 300 r/min. 1 is i_d, 2 is i_q, 3 is phase current, and 4 is rotor speed. The time scale is 200 ms/div.

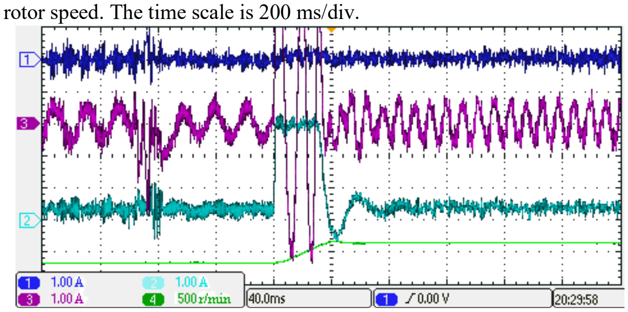

(a) Conventional FCS-MPCC

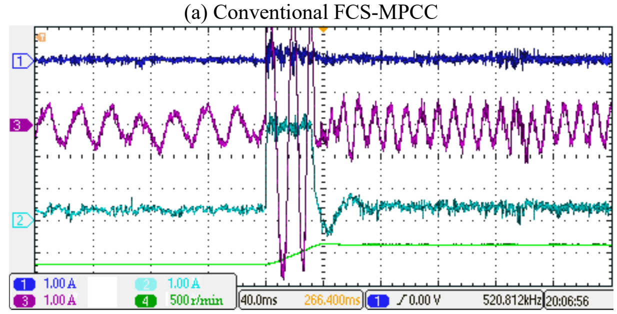

(b) Proposed FCS-MPCC

Fig. 8. Experimental results of transient state. 1 is i_d, 2 is i_q, 3 is phase current, and 4 is rotor speed. The time scale is 40 ms/div.

VI. Conclusion

In this paper, FCS-MPCC of a five-phase PMSM is analyzed. The conventional five-phase FCS-MPCC is based on virtual voltage vectors and its control set consists of 11 invariable vectors with the amplitude of $0.5527 \cdot U_{dc}$. It is not advisable to apply an invariable control set in the FCS-MPCC especially when rotor speed is low. Because a low speed leads to small back electromotive force and small voltage vectors should actually be used to control the motor. To solve the problem, this paper proposes an improved five-phase FCS-MPCC strategy with virtual voltage vectors and an adaptive control set. The amplitude of the voltage vectors in the control set is predicted in advance based on rotor speed and current references so that the control set can provide suitable vector candidates for the cost function in every control interval. What's more, to improve the transient performance, an additionally increased amplitude is adopted at transient state. Simulation and experimental results illustrate that by using the proposed algorithm, the steady performance of the proposed FCS-MPCC is largely improved while the transient response is still fast.

REFERENCES

[1] F. Barrero and M. J. Duran, "Recent Advances in the Design, Modeling, and Control of Multiphase Machines—Part I," *IEEE Trans. Ind. Electron.*, vol. 63, no. 1, pp. 449-458, Jan. 2016.

[2] W. Zhao, C. Gu, Q. Chen, J. Ji and D. Xu, "Remedial phase-angle control of a five-phase fault-tolerant permanent-magnet vernier machine with short-circuit fault," *CES Transactions on Electrical Machines and Systems*, vol. 1, no. 1, pp. 83-88, March 2017.

[3] L. Parsa and H. A. Toliyat, "Five-phase permanent-magnet motor drives," *IEEE Trans. Ind. Appl.*, vol. 41, no. 1, pp. 30-37, Jan./Feb. 2005.

[4] L. Zhang, Y. Fan, R. D. Lorenz, A. Nied and M. Cheng, "Design and comparison of three-phase and five-phase FTFSCW-IPM motor open-end winding drive systems for electric vehicles applications," *IEEE Trans. on Veh. Technol.*, vol. 67, no. 1, pp. 385-396, Jan. 2018.

[5] A. A. Ahmed, B. K. Koh and Y. I. Lee, "A Comparison of Finite Control Set and Continuous Control Set Model Predictive Control Schemes for Speed Control of Induction Motors," *IEEE Trans. Ind. Informat.*, DOI: 10.1109/TII.2017.2758393.

[6] F. Wang, X. Mei, J. Rodriguez and R. Kennel, "Model predictive control for electrical drive systems-an overview," *CES Transactions on Electrical Machines and Systems*, vol. 1, no. 3, pp. 219-230, September 2017.

[7] J. Yang, W. X. Zheng, S. Li, B. Wu and M. Cheng, "Design of a Prediction-Accuracy-Enhanced Continuous-Time MPC for Disturbed Systems via a Disturbance Observer," *IEEE Trans. Ind. Electron.*, vol. 62, no. 9, pp. 5807-5816, Sept. 2015.

[8] R. Errouissi, A. Al-Durra, S. M. Muyeen and S. Leng, "Continuous-time model predictive control of a permanent magnet synchronous motor drive with disturbance decoupling," *IET Electric Power Applications*, vol. 11, no. 5, pp. 697-706, May 2017.

[9] M. Arahal, F. Barrero, S. Toral, M. Duran, and R. Gregor, "Multiphase current control using finite-state model-predictive control," *Control Eng. Practice*, vol. 17, no. 5, pp. 579–587, May 2009.

[10] J. Rodriguez et al., "State of the Art of Finite Control Set Model Predictive Control in Power Electronics," *IEEE Trans. Ind. Informat.*, vol. 9, no. 2, pp. 1003-1016, May 2013.

[11] C. Xia, Y. Wang and T. Shi, "Implementation of Finite-State Model Predictive Control for Commutation Torque Ripple Minimization of Permanent-Magnet Brushless DC Motor," *IEEE Trans. Ind. Electron.*, vol. 60, no. 3, pp. 896-905, March 2013.

[12] C. S. Lim, E. Levi, M. Jones, N. A. Rahim and W. P. Hew, "FCS-MPC-Based Current Control of a Five-Phase Induction Motor and its Comparison with PI-PWM Control," *IEEE Trans. Ind. Electron.*, vol. 61, no. 1, pp. 149-163, Jan. 2014.

[13] F. Barrero et al., "An Enhanced Predictive Current Control Method for Asymmetrical Six-Phase Motor Drives," *IEEE Trans. Ind. Electron.*, vol. 58, no. 8, pp. 3242-3252, Aug. 2011.

[14] Y. Wang et al., "Deadbeat Model-Predictive Torque Control With Discrete Space-Vector Modulation for PMSM Drives," *IEEE Trans. Ind. Electron.*, vol. 64, no. 5, pp. 3537-3547, May 2017.

[15] D. Su, C. Zhang and Y. Dong, "Finite-State Model Predictive Current Control for Surface-Mounted Permanent Magnet Synchronous Motors Based on Current Locus," *IEEE Access*, vol. 5, pp. 27366-27375, Nov. 2017.

[16] C. Xue, W. Song and X. Feng, "Finite control-set model predictive current control of five-phase permanent-magnet synchronous machine based on virtual voltage vectors," *IET Elect. Power Appl.*, vol. 11, no. 5, pp. 836-846, May 2017.

Wusen Wang received the B.Sc. degree in electrical engineering from Southeast University, Nanjing, China, in 2016, where he is currently working toward the M.Sc. degree.

His research interests include electric machines and drives.

Ying Fan (M'07–SM'14) received the B.Sc. and M.Sc. degrees from the Department of Electrical Engineering, Nanjing University of Astronautics and Aeronautics, Nanjing, China, in 1991 and 1996, respectively, and the Ph.D. degree in electrical and electronic engineering from the University of Hong Kong, Hong Kong, in 2006.

She is currently a Professor in the School of Electrical Engineering, Southeast University, Nanjing, China. From August 2014 to September 2015, she was a Visiting Professor with the Wisconsin Electric Machines and Power Electronics Consortium, University of Wisconsin-Madison, Madison, WI, USA. She has published more than 40 technical papers and holds 20 patents in these areas. Her teaching and research interests include electric drives, electric vehicles, and wind power generation.

Siyu Chen received the B.Sc. degree in electrical engineering from Southeast University, Nanjing, China in 2015, where she is currently working toward the M.Sc. degree.

From April 2016 to September 2016, she was an exchange student with the RWTH-Aachen University in Aachen, Germany. Her research interests include electric machines and drives.

Qiushi Zhang received the B.Sc. degree in electrical engineering from Southeast University, Nanjing, China, in 2016, where he is currently working toward the M.Sc. degree.

His research interests include the predictive control and optimization control.